

Decoherence Due to Discrete Noise in Josephson Qubits

E. Paladino

*NEST-INFN & Dipartimento di Metodologie Fisiche e Chimiche (DMFCI),
Università di Catania, viale A. Doria 6,
95125 Catania, Italy & INFN UdR Catania*

L. Faoro

*Institute for Scientific Interchange (ISI) & INFN,
Viale Settimo Severo 65, 10133 Torino, Italy.*

G. Falci

*NEST-INFN & Dipartimento di Metodologie Fisiche e Chimiche (DMFCI),
Università di Catania, viale A. Doria 6,
95125 Catania, Italy & INFN UdR Catania*

Abstract

We study decoherence produced by a discrete environment on a charge Josephson qubit by introducing a model of an environment of bistable fluctuators. In particular we address the effect of $1/f$ noise where memory effects play an important role. We perform a detailed investigation of various computation procedures (single shot measurements, repeated measurements) and discuss the problem of the information needed to characterize the effect of the environment. Although in general information beyond the power spectrum is needed, in many situations this results in the knowledge of only one more microscopic parameter of the environment. This allows to determine which degrees of freedom of the environment are effective sources of decoherence in each different physical situation considered.

PACS numbers: 03.65.Yz, 03.67.Lx, 05.40.-a

A high degree of quantum coherence is crucial for operating quantum logic devices [1]. Solid state nanodevices seem particularly promising because of integrability and flexibility in the design and several possible implementations have been proposed [2, 3, 4, 5, 6]. Few recent experiments succeeded in detecting coherent dynamics in superconducting devices [7, 8, 9, 10], but revealed limitations in the performances, due to decoherence.

In a quantum logic device the interesting degrees of freedom are related to a given set of observables which we can prepare (write) and measure (read), and define the *system*. Their eigenstates $|\{q_i\}\rangle$ form the *computational basis*. The dynamics of a state $|\psi, t\rangle = \sum_{q_1 \dots q_N} c_{q_1 \dots q_N}(t) |q_1, \dots, q_N\rangle$ may be controlled if the Hamiltonian of the system is tunable. Loss of coherence is due to the fact that the Hilbert space of the device is much larger than the computational space [11, 12]. The additional degrees of freedom define the *environment*, which cannot be controlled and moreover little information is available on it. Decoherence is ultimately due to the entanglement between system and environment [11], but in order to pursue this point of view one should be able to study the full dynamics, in particular system-environment correlations. A less fundamental point of view, which we adopt here, is to associate decoherence to the loss of fidelity of a quantum gate. The environment blurs the output signal because it produces uncertainties in the phase relation between the amplitudes, $c_{\{q_i\}}(t)$.

The environment degrees of freedom may be “internal” to the device, which is a many-body object, or “external”, belonging to the circuitry and to auxiliary devices. Internal decoherence is a serious problem in solid state nanodevices, due to the presence of many low energy excitations.

Investigation of the reduced qubit dynamics requires information about the environment. In several cases (weakly coupled environment [13], harmonic oscillator environment [14, 15]) the information is contained in the power spectrum of the environment operators coupled to the qubit [32]. In this work we study a more general situation, an environment of quantum bistable fluctuators which may have memory on the time scale of the qubit dynamics, and may display the effect of non-gaussian correlations. A physical example are charged impurities in substrates and oxides. These background charges (BC) produce for instance the $1/f$ noise [17] observed in metallic tunnel junctions [18, 19].

We will present here analytic results which elucidate several aspects of the BCs environment. In particular we show that decoherence depends on details of the dynamics of the

environment beyond the power spectrum [20]. As a consequence it may differ for different gates, but in many cases the additional information required reduces to one microscopic parameter [21].

I. MODEL FOR THE SYSTEM AND THE ENVIRONMENT

Superconducting qubits [3, 4, 5, 6] are the only solid state implementations where coherence in a single qubit has been observed in the time domain [7, 8, 9] and two-qubit systems are investigated [10]. Thus problems on decoherence can be posed in a realistic perspective. In all the above implementations it has been recognized that $1/f$ noise is a major source of decoherence. We will focus on charge-Josephson qubits [5], where $1/f$ noise produced by BCs trapped close to the device (Fig. 1). We describe these BCs by introducing an impurity model. Many of our results and methods can be applied to different noise sources (eg. flux noise in flux-Josephson qubits [22, 23]) and other solid-state implementations (eg. gates based on the Coulomb interaction in semiconductor-spin qubits), but we will not discuss these topics here.

A. The Superconducting Box

The charge-Josephson qubit [5] is a superconducting island connected to a circuit via a Josephson junction and a capacitance C_2 (Fig. 1). The computational states are associated with the charge Q in the island. They are mixed by the Josephson tunneling. Level splittings can be tuned by the external voltage V_x and under suitable conditions ($E_C \gg E_J$ and low temperatures $k_B T \ll E_J$) only two charge states are important, which define the z component of a pseudospin. The the system implements a qubit with Hamiltonian

$$\mathcal{H}_Q = \frac{\varepsilon}{2} \sigma_z - \frac{E_J}{2} \sigma_x \quad ; \quad \varepsilon(V_x) = 4E_C(1 - C_2 V_x/e) \quad (1)$$

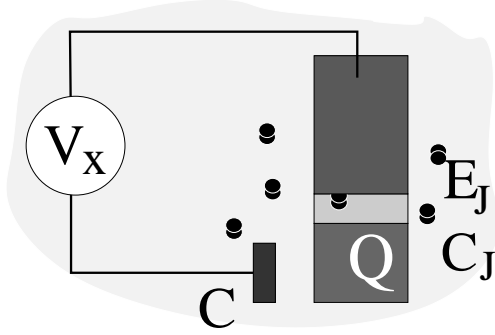


FIG. 1: A charge Josephson qubit in the presence of BCs located in the substrate or in the oxide close to the junction. Relevant scales are the charging energy $E_C = e^2/2(C_1 + C_2)$ and the Josephson energy E_J

B. System Plus Environment Hamiltonian

We describe each BC as a localized impurity level connected to a fermionic band [20, 24, 25]. For a single impurity the total Hamiltonian is

$$\mathcal{H} = \mathcal{H}_Q - \frac{v}{2} b^\dagger b \sigma_z + \mathcal{H}^I ; \quad \mathcal{H}^I = \varepsilon_c b^\dagger b + \sum_k [T_k c_k^\dagger b + \text{h.c.}] + \sum_k \varepsilon_k c_k^\dagger c_k \quad (2)$$

Here \mathcal{H}^I describes the BC alone: b (b^\dagger) destroys (creates) an electron in the localized level ε_c and the electron may tunnel with amplitude T_k to a band, described by the operators c_k , c_k^\dagger and the energies ε_k . An important scale is the switching rate $\gamma = 2\pi\mathcal{N}(\varepsilon_c)|T|^2$ (\mathcal{N} is the density of states of the band, and $|T_k|^2 \approx |T|^2$), which characterizes the relaxation regime of the BC. The BC determines a bistable extra bias v for the qubit, via the coupling term. For a set of BCs we generalize Eq. (2) as follows

$$\mathcal{H} = \mathcal{H}_Q - \frac{1}{2} \hat{E} \sigma_z + \sum_i \mathcal{H}_i^I \quad (3)$$

where extra bias operator is $\hat{E}(t) = \sum_i v_i b_i^\dagger b_i$. For simplicity the assumption that each localized level is connected to a distinct band has been made.

C. Model for $1/f$ Noise

The environment in Eq. (3) above is specified by the distribution of the switching rates γ_i which we choose in order to reproduce the $1/f$ noise. The standard way [17] is to assume

a distribution $P(\gamma) \propto 1/\gamma$ for $\gamma \in [\gamma_m, \gamma_M]$. Indeed if we look at the relaxation regime of the BC, the total extra polarization is a classical stochastic process $E(t)$ with power spectrum

$$S(\omega) = \sum_i S_i(\omega) \quad ; \quad S_i(\omega) = \frac{1}{2} v_i^2 (1 - \overline{\delta p^2}) \frac{\gamma_i}{(\gamma_i^2 + \omega^2)} \quad , \quad (4)$$

$\overline{\delta p}$ being the thermal average of the difference in the populations of the two states of the BC, the distribution $P(\gamma)$ leads to to $1/f$ noise, $S(\omega) = \{\pi(1 - \overline{p^2}) n_d \overline{v^2}/(4 \ln 10)\} \omega^{-1}$ for frequencies $\omega \in [\gamma_m, \gamma_M]$ (n_d is the number of fluctuators per noise decade). With the above choice of parameters, the Hamiltonian Eq. (3) has been used to study decoherence due to $1/f$ noise [20].

II. REDUCED DYNAMICS

Our aim is to investigate the effect of the BC environment on the dynamics of the qubit. The standard road-map is to calculate the reduced density matrix [14] of the qubit $\rho^Q(t) = \text{Tr}_E\{W(t)\}$, $W(t)$ being the full density matrix. In the standard weak coupling approach a master equation for $\rho^Q(t)$ is written [13], the environment entering its dynamics only via the power spectrum, Eq. (4). A master equation for $\rho^Q(t)$ can also be obtained by modeling the environment by a set of harmonic oscillators. By using diagrammatic techniques [14, 26, 27] results of the standard weak coupling approach are obtained at lowest order in the couplings v , but it has been pointed out that higher orders are important for a $1/f$ oscillator environment [20, 27, 28].

The failure of the standard weak coupling approach is due to the fact that the $1/f$ environment includes fluctuators which are very slow on the time scale of the reduced dynamics, the approach being reliable only for BCs with $v_i \ll \gamma_i$ [13, 20]. Rather than study higher orders in the perturbation series [27], we prefer to use a different strategy. We study the models Eqs.(2,3) by enlarging the system and considering only the bands as the environment. The modified road-map consists in calculating in some approximation the reduced density matrix (RDM) $\rho(t) = \text{Tr}_{bands}\{W(t)\}$ and then extract exactly $\rho^Q(t)$. This allows to obtain results to all orders in the coupling v and to investigate details of various quantum gates. The disadvantage is that we have a larger system to deal with. We have investigated this problem with different techniques [20], here we present a master equation approach, which covers many of the results we obtained before.

A. Master Equation for a Single BC

We split Eq. (2) in system, $\mathcal{H}_0 = \mathcal{H}_Q - \frac{v}{2} b^\dagger b \sigma_z + \varepsilon_c b^\dagger b$, and environment, $\mathcal{H}_E = \sum_k \varepsilon_k c_k^\dagger c_k$, coupled by $\mathcal{V} = \sum_k [T_k c_k^\dagger b + \text{h.c.}]$. The eigenstates (and eigenvalues) of \mathcal{H}_0 are product states of the form $|qubit\rangle |BC\rangle$, namely $|a\rangle = |\theta+\rangle |0\rangle$ ($-\Omega/2$), $|b\rangle = |\theta-\rangle |0\rangle$ ($\Omega/2$), $|c\rangle = |\theta'+\rangle |1\rangle$ ($-\Omega'/2 + \varepsilon_c$), $|d\rangle = |\theta'-\rangle |1\rangle$ ($\Omega'/2 + \varepsilon_c$). Here $|\theta\pm\rangle$ are the two eigenstates of $\sigma_{\mathbf{n}}$, the direction being specified by the polar angles θ and $\phi = 0$. Each set of qubit states corresponds to a value of $b^\dagger b = 0, 1$: the two level splittings are $\Omega = \sqrt{\varepsilon^2 + E_J^2}$ and $\Omega' = \sqrt{(\varepsilon + v)^2 + E_J^2}$, and finally $\cos \theta = \varepsilon/\Omega$, $\sin \theta = E_J/\Omega$, $\cos \theta' = (\varepsilon + v)/\Omega'$, $\sin \theta' = E_J/\Omega'$.

In the basis of the eigenstates of \mathcal{H}_0 the master equation for the RDM in the Schrödinger representation reads

$$\frac{d\rho_{ij}(t)}{dt} = -i\omega_{ij}\rho_{ij}(t) + \sum_{mn} R_{ijmn}\rho_{mn}(t) \quad (5)$$

where ω_{ij} is the difference of the eigenenergies and R_{ijmn} are the elements of the Redfield tensor [13]

$$R_{ijmn} = \int_0^\infty d\tau \left\{ C_{njmi}^>(\tau) e^{i\omega_{mi}\tau} + C_{njmi}^<(\tau) e^{i\omega_{jn}\tau} - \delta_{nj} \sum_k C_{ikmk}^>(\tau) e^{i\omega_{mk}\tau} - \delta_{im} \sum_k C_{nkjk}^<(\tau) e^{i\omega_{kn}\tau} \right\} \quad (6)$$

The correlation functions are given by

$$C_{ijkl}^{\gtrless}(t) = [\langle i|b|j\rangle \langle l|b^\dagger|k\rangle + \langle i|b^\dagger|j\rangle \langle l|b|k\rangle] iG^{\gtrless}(t)$$

where $iG^>(\omega) = \gamma/(1 + e^{-\beta\omega})$, $G^<(\omega) = G^>(-\omega)$. Many of the coefficients R_{ijmn} vanish. In particular the system of equations (5) splits in two blocks. The first contains the populations and the coherences ρ_{ab} and ρ_{cd} , together with their conjugate, i.e. the elements diagonal in the BC. The second block contains all the other coherences, which vanish identically if the initial RDM $\rho(0)$ is diagonal in the BC, the physically relevant case for our purposes.

In the standard secular approximation [13] in the r.h.s. of Eq. (5) are retained only terms with coefficients R_{ijij} , but this is not enough in our problem. To discuss possible approximations we first point out that we are interested in the case $v \ll \Omega, \Omega'$. We have two important scales, namely $\Omega' - \Omega$ and $\Omega \sim \Omega'$, the latter being much larger than the former. The secular approximation is valid if $\gamma \ll \Omega' - \Omega$, i.e. for an almost static BC. If

$\gamma \sim \Omega' - \Omega \ll \Omega \sim \Omega'$ we can no longer neglect the coefficients mixing ρ_{ab} and ρ_{cd} (and those mixing the conjugates). We call this regime adiabatic. Finally in the fast BC regime, $\gamma \gtrsim \Omega, \Omega'$, all the $R_{ij\,mn}$ must be present. Despite of this, the reduced dynamics of the qubit is just the result of lowest order approach [14, 26, 27], so we will not discuss this regime anymore.

B. Results for Adiabatic BCs

In the adiabatic regime coherences are calculated using the following elements of the Redfield tensor

$$\begin{aligned} R_{abab} &= -\frac{\gamma}{2} [1 - c^2\delta - s^2\delta' + i(c^2w + s^2w')] \quad ; \quad R_{abcd} = \frac{c^2\gamma}{2} (1 + \delta - iw) \\ R_{cdcd} &= -\frac{\gamma}{2} (1 + c^2\delta + s^2\delta' + i(c^2w - s^2w')) \quad ; \quad R_{cdab} = \frac{c^2\gamma}{2} (1 - \delta - iw) \end{aligned}$$

where $c = \cos[(\theta - \theta')/2]$, $s = \sin[(\theta - \theta')/2]$, $\delta = t_{ca} + t_{db}$, $\delta' = t_{da} + t_{cb}$, $w = w_{ca} - w_{db}$, $w' = w_{da} - w_{cb}$ and

$$t_{ij} = \frac{1}{2} \operatorname{tgh} \left(\frac{\beta\omega_{ij}}{2} \right) \quad ; \quad w_{ij} = -\frac{1}{\pi} \Re \left\{ \psi \left(\frac{\pi + i\beta\omega_{ij}}{2\pi} \right) \right\}.$$

Here $\psi(z)$ is the digamma function. The coherences $\rho_{ab}(t)$ and $\rho_{cd}(t)$ can be found in closed form by simply diagonalizing a 2×2 matrix. They allow to study the qubit coherence via $\langle \sigma_y(t) \rangle = -2\Im[\rho_{ab}(t) + \rho_{cd}(t)]$. The qubit coherence decays as $\exp\{-\Gamma(t)\}$, where

$$\Gamma(t) = - \ln \left| \frac{\rho_{ab}(t) + \rho_{cd}(t)}{\rho_{ab}(0) + \rho_{cd}(0)} \right|. \quad (7)$$

Here we present the analytic solution in a regime where the dynamics of the charge is not modified by the presence of the qubit, a case which is of interest for $1/f$ noise. We find

$$\rho_{ab}(t) + \rho_{cd}(t) = e^{i(\Omega + \gamma g/2)t} \frac{1}{2\alpha} \left\{ A(\alpha) e^{-\frac{\gamma}{2}(1-\alpha)t} - A(-\alpha) e^{-\frac{\gamma}{2}(1+\alpha)t} \right\} \quad (8)$$

where $\alpha = \sqrt{1 - g^2 - 2ig\bar{\delta p} - (1 - c^4)(1 - \bar{\delta p}^2)}$ and $g = (\Omega' - \Omega)/\gamma$ enter the decay rates whereas the prefactors are

$$A(\alpha) = (\alpha + c^2 - ig') \rho_{ab}(0) + (\alpha + c^2 + ig') \rho_{cd}(0) \quad ; \quad g' = g + i\bar{\delta p}(1 - c^2).$$

C. Two Regimes for the BC

A rough analysis of Eq. (8) allows to draw a physical picture. If $g \gg 1$, α is substantially imaginary, reflecting the fact that a very slow BC mainly provides a static energy shift. Instead for $g \ll 1$ the decay rates acquire a real part thus a fast BC may determine an exponential reduction of the output signal. From a more quantitative analysis [20] it emerges that BCs with $g \ll 1$, which we call *weakly coupled*, behave as a suitable set of harmonic oscillators with power spectrum given by Eq. (4). They mainly produce the homogeneous broadening of the signal. Instead BCs with $g \gg 1$, which we call *strongly coupled*, give rise to memory effects and deviations of their statistical properties from those of an oscillator environment (cumulants higher than the second) are relevant [17]. They mainly produce the inhomogeneous broadening of the signal.

Finally we compare this result with other approaches. Notice first that Eq. (8) is valid if the power spectrum $S_i(\omega)$ (see Eq. (4)) is negligible at frequencies $\omega \sim \Omega$. In this regime both the decay $\Gamma(t)$ Eq. (7) and the energy shift reproduce the results of the standard weak coupling approach [13] if $\gamma t \gg 1$. On the other hand, as in the work of Refs. [14, 26, 27], we may simulate the effect of the BC by a suitable set of quantum harmonic oscillators. The resulting decoherence rate for this oscillator environment is given by

$$\Gamma_{osc}(t) = \frac{1}{2} g^2 \left[\frac{\partial^2 \Gamma(t)}{\partial g^2} \right]_{g=0} \quad (9)$$

where $\Gamma(t)$ is given by Eq. (8) with thermal initial conditions for the BC.

III. PURE DEPHASING

For $E_J = 0$ the environment only produces random fluctuations of the level splitting. This case, usually referred to as “pure dephasing”, is special in that the Hamiltonian (3) commutes with σ_z . The charge in the island is then conserved and no relaxation occurs, but if we prepare the qubit in a superposition the system will dephase.

If the initial density matrix is factorized, $W(0) = w_E(0) \otimes \rho^Q(0)$, it is possible to write an exact expression for the coherences only in terms of the environment [12, 20, 21],

$$\rho_{01}^Q(t) = \rho_{01}^Q(0) e^{-\Gamma(t) - i\delta E(t)} ; \quad \Gamma(t) = -\ln |\text{Tr}_E \{ w_E(0) e^{i\mathcal{H}_{-1}t} e^{-i\mathcal{H}_1 t} \}| \quad (10)$$

where $\mathcal{H}_\eta = \sum_i \mathcal{H}_i^I - (\eta/2) \hat{E}$. This general expression may be further simplified because individual charges contribute independently to $\Gamma(t)$, $\Gamma(t) = \sum_i \Gamma_i(t)$, where $\Gamma_i(t)$ is the dephasing due to a single charge resulting from the Hamiltonian Eq. (2). We notice that in this case $\theta = \theta'$, which implies that $\rho_{10}^Q(t) = \rho_{ab}(t) + \rho_{cd}(t)$ and moreover the adiabatic approximation is exact, since the Redfield coefficients relating the above two coherences with all the other entries of the RDM vanish identically. Then $\Gamma_i(t)$ is given by Eq. (7) and in the limit described by Eq. (8) we find the analytic form

$$\Gamma_i(t) = -\ln \left| A_i e^{-\frac{\gamma_i}{2}(1-\alpha_i)t} + (1 - A_i) e^{-\frac{\gamma_i}{2}(1+\alpha_i)t} \right| \quad (11)$$

where $A_i = [1 + (1 - ig_i)/\alpha] p_{0i} + [1 + (1 + ig_i)/\alpha] p_{1i}$, $g_i = v_i/\gamma_i$, $\alpha_i = \sqrt{1 - g_i^2 - 2ig_i\overline{\delta p_i}}$, and p_{0i} (p_{1i}) is the probability that the i -th BC is initially empty (singly occupied). This result has been obtained using several different techniques in [20, 21].

Finally by combining the equations of this section with Eq. (9) we recover the exact result of a set of harmonic oscillators [12]

$$\Gamma_{osc}(t) = \int_0^\infty \frac{d\omega}{\pi} S(\omega) \frac{1 - \cos \omega t}{\omega^2}. \quad (12)$$

A. Single BC

We study deviations of Eq. (11) from the result for an oscillator environment, Eq. (12). We consider different initial conditions for the BCs. Substantial deviations are clearly observed, except in the case of a weakly coupled BC ($g = 0.1$). In particular BCs with $g > 1$ induce slower dephasing compared to an oscillator environment with the same $S(\omega)$, a sort of saturation effect. Recurrences at times comparable with $1/v$ are visible in $\Gamma(t)$. In addition strongly coupled charges show memory effects. We now study the effect of the initial conditions of the BC, expressed via $\delta p_0 = p_0 - p_1$. In a single shot process $\delta p_0 = \pm 1$ and $\Gamma(t)$ describes dephasing *during* time evolution (homogeneous broadening). Memory effects are apparent and in particular for $\gamma t \ll 1$ the short time behavior is $\Gamma(t) \approx v^2 t^2 (1 - \delta p_0^2)/8 + \gamma v^2 t^3 (1 + 2\delta p_0 \overline{\delta p} - 3\delta p_0^2)/24 \propto t^3$. A two level system is stiffer than a set of oscillators and indeed $\Gamma_{osc}(t) \approx v^2 (1 - \overline{\delta p}^2)/8 t^2$. On the other hand if we choose $\delta p_0 = \overline{\delta p}$ in Eq. (11), for very short times $\Gamma(t) \approx \Gamma_{osc}(t)$. This case corresponds physically to repeated measurements where the preparation of the BC is not controlled and

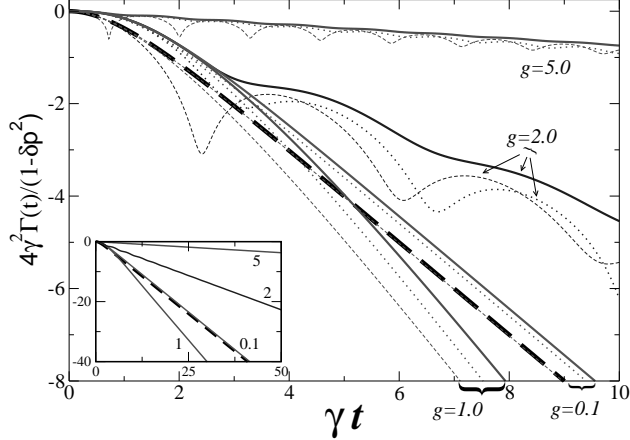


FIG. 2: Reduced $\Gamma(t)$ due to a BC prepared in a stable state ($\delta p_0 = 1$ solid lines and $\delta p_0 = -1$ dotted lines) and in a thermal mixture ($\delta p_0 = \overline{\delta p}$ dashed lines) for the indicated values of $g = v/\gamma$. Inset: longer time behavior for stable state preparation. The curves are normalized in such a way that the oscillator approximation for all of them coincides (thick dashed line)

determines slightly different characteristic frequency for the qubit. This sort of inhomogeneous broadening adds to decoherence during the individual time evolutions and determines a faster decay of $\Gamma(t)$.

To summarize a weakly coupled BC, $g \ll 1$, behaves as a source of gaussian noise, decoherence depending only on the power spectrum of the fluctuator, whereas decoherence due a strongly coupled BC, $g \gg 1$, displays saturation effects and dependence on the initial conditions of the BC.

B. $1/f$ Noise in Single Shot Measurements

The set of BCs producing $1/f$ noise contains both weakly and strongly coupled fluctuators, so no typical time scale is present. A very large number of slow fluctuators is present, and it is not a priori clear how saturation manifests. In Fig. 3 we show the results for a realistic sample. We choose initial conditions $\delta p_{0j} = \pm 1$ randomly distributed on the set of N BCs with $(1/N) \sum_j \delta p_{0j} \approx \overline{\delta p}$. We checked that different microscopic realizations of this conditions give roughly the same total initial extra bias $E(0)$ and the same dephasing. We calculate dephasing during the time evolution, i.e. the average signal of several single-shot experiments, where $E(0)$ is re-calibrated before each experiment. This ideal protocol

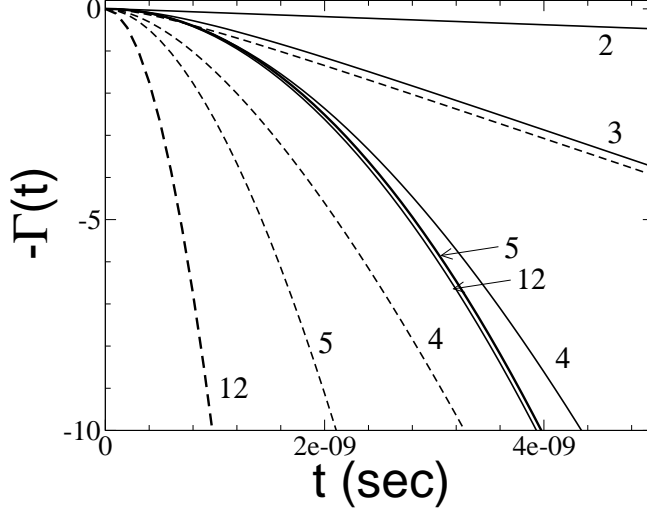


FIG. 3: $\Gamma(t)$ due to $1/f$ noise in the range $\omega \in [\gamma_m, 10^{12} \text{ Hz}]$, for decreasing γ_m (solid lines, the label is the number of decades included). Slower BCs saturate whereas this not happens for an oscillator environment (dashed lines). Parameters ($\bar{v} = 9.2 \times 10^7 \text{ Hz}$, $n_d = 1000$) give the experimental noise levels and reproduce the observed decay of the echo signal [19]. Couplings v_i are distributed with $\Delta v/\bar{v} = 0.2$

minimizes the effects of the environment.

We now perform a spectral analysis of the effects of the environment by adding slower fluctuators decade after decade, in a way such that $1/f$ noise with the same amplitude \mathcal{A} is present for $\omega \in [\gamma_m, 10^{12} \text{ Hz}]$. We see in this example that dephasing is given by BCs with $\gamma_j > 10^7 \text{ Hz} \approx \bar{v}/10$. The overall effect of the strongly coupled BCs ($\gamma_j < \bar{v}/10$) is minimal, despite of their large number, thus low-frequency noise saturates. Instead $\Gamma_{osc}(t)$, Eq. (12) does not saturate at low frequencies. We notice finally that for this protocol $\Gamma(t)$ is roughly given by $\Gamma_{osc}(t)$ provided low frequencies are cut off at $\omega \sim \bar{v}$. Thus dephasing depends essentially on a single additional parameter besides the power spectrum $S(\omega)$, namely the average coupling \bar{v} or equivalently the number of charges producing a decade of noise, n_d .

Our results are not very sensitive to the value of n_d we choose. Indeed for constant amplitude \mathcal{A} we must keep constant $\sum_i v_i^2 \approx n_d \bar{v}^2$, so the effective low-frequency cutoff $\sim \bar{v}$ varies as $n_d^{-1/2}$. For $n_d \rightarrow \infty$ the low-frequency cutoff goes to zero, as in the result Eq. (12) for the oscillator environment.

C. Repeated Measurements and Inhomogeneous Broadening

Single-shot measurements are a goal for experimental research, but presently available protocols involve repeated measurements. For instance in [7, 19] the time evolution procedure is repeated $\sim 10^5$ times and the total current due to the possible presence of the extra Cooper pair in all the repetitions is measured. The signal is then the sum over different possible time evolutions of the BCs with initial conditions which are also randomly fluctuating. This additional blurring of the output signal results in a faster decay for $\Gamma(t)$. As explained in [21], this is accounted for by letting in $\Gamma(t)$ (i.e. in Eqs.(11)) $\delta p_{0i} = \overline{\delta p_i}(t_m)$,

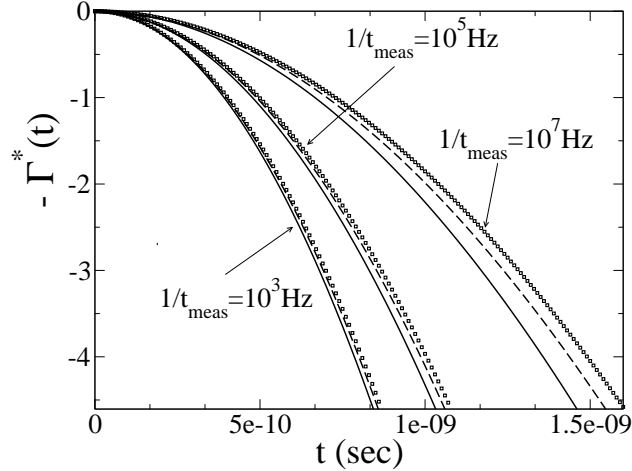


FIG. 4: Different averages over δp_{0j} for $1/f$ spectrum reproduce the effect of repeated measurements. They are obtained by neglecting (dotted lines) or account for (solid lines) the strongly correlated dynamics of $1/f$ noise. The noise level of [19] is used, by setting $\overline{|v|} = 9.2 \times 10^6 Hz$, $n_d = 10^5$, $\gamma_m = 1Hz$, $\gamma_M = 10^9 Hz$. Dashed lines are the oscillator approximation with a lower cutoff at $\omega = \min\{\overline{|v|}, 1/t_m\}$

the average of the values of δp_j sampled at regular times t_α for the overall measurement time t_m . As a rough estimate we let $\overline{\delta p_i}(t_m) = \pm 1$ if $\gamma_i t_m < 1$ and $\overline{\delta p_i}(t_m) = \overline{\delta p_i}$ for $\gamma_i t_m > 1$, and consider only the case of long overall measurement time $\overline{|v|} t_m \gg 1$. In this case BCs with $\gamma < 1/t_m$ are saturated and are not effective, whereas for the other BCs, being averaged, we may take $\Gamma^{(i)}(t) \approx \Gamma_{osc}^{(i)}(t)$ for small enough times. The result would be $\Gamma(t) \approx \int_{1/t_m}^{\infty} d\omega S(\omega)(1 - \cos \omega t)/(\pi \omega^2)$ and would proof the recipe proposed by Cottet et al. [28].

In Fig. 4, (dotted lines) we show that indeed dephasing calculated as outlined above, is roughly given at short times by the oscillator environment approximation with a lower cutoff taken at $\omega \approx \min\{|\overline{v}|, 1/t_m\}$. We also show results with a different averaging procedure $\delta p_j^0(t_m) = 1/t_m \int_0^{t_m} dt \overline{\delta p(t)}$ which takes into account the strongly correlated dynamics of $1/f$ noise (solid lines in Fig. 4.). These correlations do not affect the results except possibly for $t_m \approx |\overline{v}|$.

D. Charge Echo

Echo-type techniques have been recently suggested [7, 28] and experimentally tested [19] as a tool to reduce inhomogeneous broadening due to the low-frequency fluctuators of the $1/f$ spectrum. In the experiment of [19] the echo protocol consists of a $\pi/2$ preparation pulse, a π swap pulse and a $\pi/2$ measurement pulse. Each pulse is separated by the delay time t . We calculated the decay of the echo signal using a semi-classical approach [21, 29]. This result allowed to estimate the parameters we have used in this work by comparing with [19].

The decay depends very weakly on initial conditions of the BCs and is well reproduced by the oscillator environment approximation. This means that in the experiment [19] the echo procedure actually cancels the effect of strongly coupled charges, this conclusion being valid as long as the delay time is short, $t|\overline{v}| \ll 1$. We remark that in the regime of parameters we consider, for given noise amplitude the echo signal is strongly dependent on the high frequency cutoff and a detailed analysis may give information on the actual existence of BCs switching at rates comparable with $\Omega \sim 10$ GHz.

IV. DECOHERENCE FOR A GENERIC WORKING POINT

The most effective strategy for defeating $1/f$ noise has been implemented in the experiment by Vion et al. [8]. It is useful to explain it in a non pictorial way by considering decoherence as given by the weak coupling approach [13, 14, 26]

$$\Gamma_0(t) = \left[\frac{1}{2} S(0) \cos^2 \theta + \frac{1}{4} S(\Omega) \sin^2 \theta \right] t. \quad (13)$$

Even if this formula does not hold for $1/f$ noise, it indicates that the dangerous adiabatic term containing $S(0)$ may be eliminated (in lowest order) if one operates at $\theta = \pi/2$.

Small deviations from this point may determine a dramatic increase of decoherence [8]. Understanding decoherence in a generic operating point may help in designing more flexible gates, or to implement different strategies as computation with geometric phases [6].

A. Single BC

First we consider Eq. (8) and we notice that by changing the working point θ , a strongly coupled BC may become weakly coupled and vice-versa. For simplicity we let $KT \gg \varepsilon_c$, then $\alpha \approx \sqrt{c^4 - g^2}$. The BC is weakly coupled if $\gamma \gg \gamma_c = (\Omega' - \Omega)/c^2$. Thus, the threshold value decreases if we go from $\theta = 0$ to $\theta = \pi/2$ (see Fig. IV).

To get some insight in the problem of decoherence away from $\theta = \pi/2$ we consider $\Gamma(t)$ in the adiabatic regime Eqs. (7,8). Results plotted in Fig. 6 show $\Gamma(t)$ parametrized by θ for four values of the parameter v/γ . For reference we plot also (dashed lines) $\Gamma_0(t)$, Eq. (13). The top left panel shows a weakly coupled BC for which $\Gamma(t)$ roughly follows $\Gamma_0(t)$. The other panels show BCs with $v \geq \gamma$ which turn from strongly coupled to weakly coupled increasing $\theta \in [0, \pi/2]$. For these latter BCs saturation is less effective in suppressing decoherence when the operation point is close to $\theta = \pi/2$, which may be an indication of the fact that their effect is more sensitive to deviations from the optimal point.

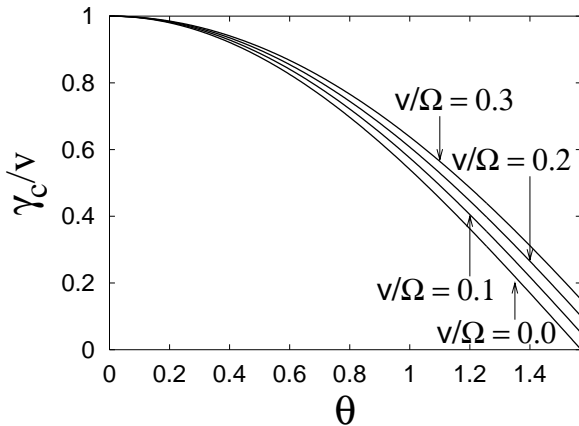


FIG. 5: The threshold value for a BC behaving as weakly coupled depends on the operating point

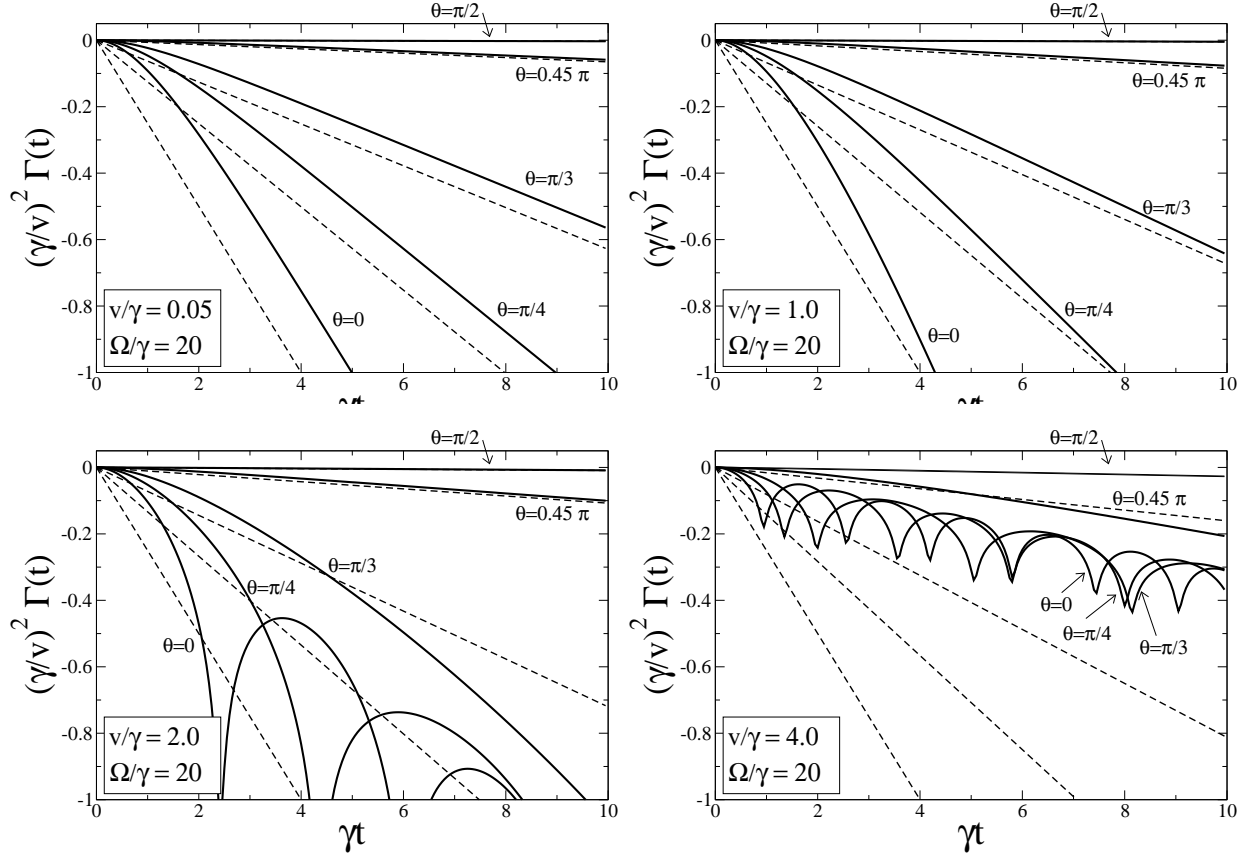


FIG. 6: Reduced $\Gamma(t)$ (solid lines) plotted for various $v/\gamma = 0.05, 1.0, 2.0, 4.0$. In each panel curves correspond, from top to bottom, to $\theta = \pi/2, 0.45\pi, \pi/3, \pi/4, 0$. For comparison $\Gamma_0(t)$ is also plotted (dashed lines). In the units used, $\Gamma_0(t)$ is the same in each panel

B. $1/f$ Noise at the Optimal Point

For a set of BCs the road-map for the reduced dynamics outlined in Sec. II is not easily implemented by generalizing the master equation Eq. (5). In [20] we used the Heisenberg equations of motion, where we factorize correlations between the qubit and the bands, and between different BCs. We are left with a set of $3(N + 1)$ coupled differential equations, where N is the total number of BCs. These approximations are expected to work for small v_i but in effect they give accurate results for general values of g_i even if v_i/E_J is not very small, as we checked by comparing with numerical evaluation of the master equation for the qubit with one and two BCs. We study decoherence at the optimal point $\theta = \pi/2$ ($\Omega = E_J$) via the Fourier transform of $\langle \sigma_z(t) \rangle$. We consider a set of weakly coupled BCs in the range $[10^{-2}, 10] E_J$ which determines $1/f$ noise around the operating frequency with amplitude

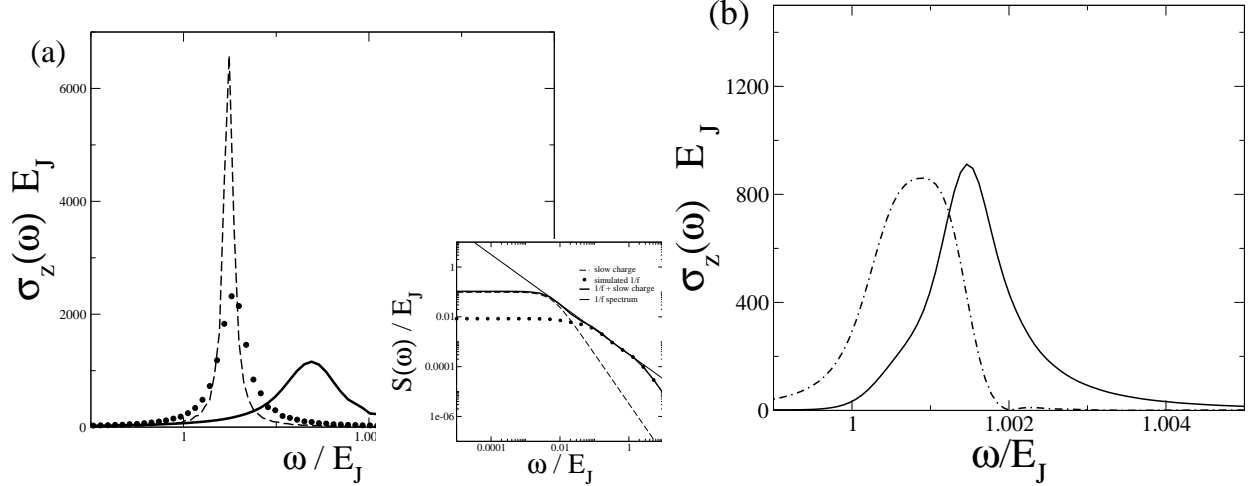


FIG. 7: (a) The Fourier transform $\sigma_z(\omega)$ for a set of weakly coupled BCs plus a single strongly coupled BC (solid line). The separate effect of the coupled slow BC alone ($g_0 = 8.3$, dashed line) and of the set of weakly coupled BCs (dotted line), is shown for comparison. In the inset the corresponding power spectra: notice that at $\omega = E_J$ the power spectrum of the extra charge alone (dashed line) is very small. In all cases the noise level at E_J is fixed to the value $S(E_J)/E_J \approx 3.18 \times 10^{-4}$. (b) The Fourier transform $\sigma_z(\omega)$ for a set of weakly coupled BCs plus a strongly coupled BC ($v_0/\gamma_0 = 61.25$) prepared in the ground (dotted line) or in the excited state (thick line)

of the typical measured spectra [18, 19] extrapolated at GHz frequencies. Dephasing due to this set of BCs agrees with the weak coupling result Eq. (13). Then we add a slower (and strongly coupled $g_0 = v_0/\gamma_0 = 8.3$) BC, which should produce no effect according to Eq. (13), Fig. 7a. We find that the strongly coupled BC alone determines a dephasing rate comparable with that of the weakly coupled BCs and the overall dephasing rate is more than doubled. This result shows that slower charges $\gamma \ll \Omega$ play a role in dephasing. Moreover information beyond $S(\omega)$ is needed, as we checked by showing that sets of charges with different N and v_i but the same $S(\omega)$ yield substantially different values of the decoherence rate. Decoherence is larger if BCs with $g \gtrsim 1$ are present in the set. In summary these results show that Eq. (13) *underestimates* the effect of strongly coupled BCs and also that decoherence at the optimal point may be substantial even if the $1/f$ spectrum does not extend up to frequencies $\sim E_J$.

If we further slow down the added BC we find that Γ_ϕ increases toward values $\sim \gamma_0$,

the switching rate of the BC. This indicates that the effect of strongly coupled BCs on decoherence tends to saturate, in analogy with the results for pure dephasing. In this regime, we observe also memory effects related to the initial preparation of the strongly coupled BC (see Fig. 7b). Again we expect a dependence of dephasing on the protocol of the quantum gate.

V. CONCLUSIONS

In conclusion we have studied dephasing due to charge fluctuations in solid state qubits. For a fluctuator environment with $1/f$ spectrum memory effects and higher order moments are important so additional information on the environment is needed to estimate dephasing. In this case the additional information of the environment needed depends on the protocol but often reduces to a single parameter. A new energy scale emerges, the average coupling $\overline{|v|}$ of the qubit with the BCs, which is the additional information needed to discuss single shot experiments (alternatively one should know the order of magnitude of n_d). For repeated experiments the relevant scale is instead $\min\{\overline{|v|}, 1/t_m\}$ where t_m is the overall measurement time. We point out that these scales emerge directly from the study of the dynamics of the model, and not from further assumptions. Finally echo measurements are sensitive to the high-frequency cutoff γ_M of the $1/f$ spectrum.

It is interesting to notice that some result relative to an environment of quantum harmonic oscillators for arbitrary qubit-environment coupling may be obtained as a limit of the discrete environment in the semi-classical regime, and depend on the classical statistical properties of an equivalent random process with no reference to the quantum nature of the environment.

Our results are directly applicable to other implementations of solid state qubits. Josephson flux qubits [22, 30] suffer from similar $1/f$ noise, originated from trapped vortices. Our model applies if σ_z represents the flux. Also the parametric effect of $1/f$ noise on the coupling energy of a Josephson junction [23] can be analyzed within our model, as long as individual fluctuators do not determine large variations of E_J . In this case it may be possible that the same sources generate both charge noise and fluctuations of E_J . This can be accounted for by choosing the “noise axis” as the \hat{z} axis.

An important issue is to understand dephasing near the optimal operating points of the qubit [8]. Low-frequency noise can also be minimized by echo techniques, but the flexibility

in the implementation of gates is greatly reduced. A possibility is to implement quantum computation using Berry phases [6], where the design of gates includes an echo procedure. Frequency shifts can be calculated within our model but a reliable analysis of the effect of $1/f$ noise is still missing.

Finally we mention that the sensitivity of coherent devices may be used to investigate high frequency noise [31]. In particular an accurate matching between measured inhomogeneous broadening, echo signal and relaxation may give reliable information on the actual existence of BCs at GHz and on the high-frequency cutoff of the $1/f$ spectrum.

Acknowledgments

We thank M. Palma, R. Fazio, A. Shnirman, G. Schön and C. Urbina for discussions which greatly sharpened the point of view presented in this work. Very useful discussion with J. Clarke, A. D'Arrigo, D. Esteve, F. Hekking, P. Lafarge, G. Giaquinta, M. Grifoni, D. van Harlingen, A. Mastellone, J.E. Mooji, Y. Nakamura, Y. Nazarov, F. Plastina, U. Weiss, D. Vion and A. Zorin are acknowledged.

-
- [1] A. Ekert and A. Jozsa, Rev. Mod. Phys. **68**, 733 (1996); *Quantum Computation and Quantum Information Theory*, edited by C. Macchiavello, G.M. Palma, A. Zeilinger, World Scientific (2000). M.Nielsen and I.Chuang *Quantum Computation and Quantum Communication*, Cambridge University Press, (2000). *Experimental implementation of quantum computation*, edited by R.G. Clark, Rinton Press, Princeton (2001).
 - [2] D. Loss and P. Di Vincenzo , Phys. Rev. A **57**, 120 (1998).
 - [3] Y. Makhlin, G. Schön and A. Shnirman , Rev. Mod. Phys. **73**357 (2001).
 - [4] D.A. Averin, Sol. State Comm. **105**, 659 (1998); L.B. Ioffe *et al.*, Nature **398**, 679 (1999); J.E. Mooij *et al.*, Science **285**, 1036 (1999).
 - [5] Y. Makhlin, G. Schön and A. Shnirman , Nature **398**, 305 (1999); A. Shnirman, G. Schön and Z. Hermon , Phys. Rev. Lett. **79**, 2371 (1997).
 - [6] G. Falci *et al.*, Nature **407**, 355 (2000).
 - [7] Y. Nakamura, Yu.A. Pashkin, J.S. Tsai , Nature **398**, 786 (1999).

- [8] D. Vion *et al.*, Science **296**, 886 (2002).
- [9] Y. Yu *et al.*, Science **296**, 889 (2002); J. Martinis *et al.*, Phys. Rev. Lett. **89**, 117901 (2002); J. Friedman *et al.*, Nature **406**, 43 (2000); I. Chiorescu *et al.* private communication.
- [10] Yu. A. Pashkin *et al.* cond-mat/0212314.
- [11] W. Zurek, Physics Today **44**, 36 (1991).
- [12] G.M.Palma, K.-A.Suominen and A.K.Ekert, Proc. Roy. Soc. London A **452**, 567 (1996).
- [13] C. Cohen-Tannoudji, J. Dupont-Roc and G. Grynberg *Atom-Photon Interactions*, Wiley-Interscience (1993)
- [14] U. Weiss *Quantum Dissipative Systems* 2nd Ed (World Scientific, Singapore 1999).
- [15] A. Leggett *et. al.*, Rev. Mod. Phys. **59**, 1 (1987).
- [16] A. O.Caldeira and A. J. Leggett, Ann. Phys. **149**, 374 (1983).
- [17] M.B. Weissman, Rev. Mod. Phys. **60**, 537 (1988).
- [18] A.B. Zorin *et. al.*, Phys. Rev. B **53**, 13682 (1996). M. Covington *et al.*, Phys. Rev. Lett. **84**, 5192 (2000).
- [19] Y. Nakamura *et. al.*, Phys. Rev. Lett. **88**, 047901 (2002).
- [20] E. Paladino *et. al.*, Phys. Rev. Lett. **88**, 228304 (2002).
- [21] G. Falci *et. al.*, Proceedings of the International School Enrico Fermi on "Quantum Phenomena of Mesoscopic Systems", B. Altshuler and V. Tognetti Eds., IOS Bologna (2003).
- [22] J.E. Mooij *et al.*, Science **285**, 1036 (1999).
- [23] D. J. Van Harlingen *et al.* to be published in *Quantum Computing and Quantum Bits in Mesoscopic Systems* edited by Kluwer Academic Plenum Press (2002).
- [24] R. Bauernschmitt and Y.V. Nazarov, Phys. Rev. B **47**, 9997 (1993).
- [25] G.D. Mahan *Many-Particle Physics* Kluwer Academic, New York, (2000)
- [26] M.Grifoni, E. Paladino, U. Weiss, E.Phys.J. B, **10**, 719 (1999).
- [27] A. Shnirman, Y. Makhlin, G. Schön cond-mat/0202518
- [28] A. Cottet *et al.* in *Macroscopic Quantum Coherence and Quantum Computing* edited by D.V. Averin, B. Ruggiero and P. Silvestrini, (Kluwer Pub., 2001),pg.111; E. Paladino *et. al.* ibidem, pg.359.
- [29] E. Paladino *et al.* to be published in *Quantum Computing and Quantum Bits in Mesoscopic Systems* edited by Kluwer Academic Plenum Press (2002).
- [30] L. Tian *et al.* in *Proceedings of the NATO-ASI on Quantum Mesoscopic Phenomena and*

Mesoscopic Devices in Microelectronics, edited by I.O. Kulik and R. Elliatoglu (Kluwer Pub. 2000), pg. 429.

[31] R. Aguado and L. P. Kouwenhoven, *Phys. Rev. Lett.* **84**, 1986 (2000).

[32] In this spirit the Caldeira Leggett model has been proposed to describe quantum phenomena in superconducting nanocircuits [16].